

# Decision support for the selection of reference sites using $^{137}\text{Cs}$ as soil erosion tracer

5 Laura Arata<sup>1</sup>, Katrin Meusburger<sup>1\*</sup>, Alexandra Bürgi<sup>1</sup>, Markus Zehringer<sup>2</sup>, Michael E. Ketterer<sup>3</sup>, Lionel Mabit<sup>4</sup> and Christine Alewell<sup>1</sup>

<sup>1</sup> Institute of Environmental Geosciences, Department of Environmental Sciences, University of Basel, Switzerland

<sup>2</sup> State Laboratory Basel-City, Basel, Switzerland

<sup>3</sup> Chemistry Department, Metropolitan State University of Denver, Colorado, USA

10 <sup>4</sup> Soil and Water Management & Crop Nutrition Laboratory, FAO/IAEA Agriculture & Biotechnology Laboratory, Austria.

*Correspondence to:* Katrin Meusburger (katrin.meusburger@unibas.ch)

**Abstract.** The classical approach to use  $^{137}\text{Cs}$  as soil erosion tracer is based on the comparison between stable reference sites and sites affected by soil redistribution processes, and enables to derive soil erosion and deposition rates. The method is associated with potentially large sources of uncertainty with major parts of this uncertainty being associated with the selection

15 of the reference sites. We propose a decision support tool to Check the Suitability of reference Sites (CheSS). Commonly the variation among  $^{137}\text{Cs}$  inventories of spatial replicate reference samples are taken as sole criteria to decide on the suitability of a reference inventory. Here we propose an extension of this procedure using a repeated sampling approach, where the reference sites are resampled after a certain time period. Suitable reference sites are expected to present no significant temporal variation in their decay corrected  $^{137}\text{Cs}$  depth profiles. Possible causes of variation are assessed by a decision tree. More specifically, the

20 decision tree tests for (i) uncertainty connected to small scale variability of  $^{137}\text{Cs}$  due to its heterogeneous initial fallout (such as in areas affected by the Chernobyl fallout), (ii) signs of erosion/deposition processes, (iii) artefacts due to the collection, preparation and measurement of the samples and (iv) finally, if none of the above can be assigned, this variation might be attributed to “turbation” processes (e.g. bioturbation, cryoturbation and mechanical turbation such as avalanches or rock falls).

25 CheSS was exemplarily applied in one Swiss alpine valley, where the apparent temporal variability was questioning the suitability of selected reference sites. In general we suggest the application of CheSS to implement first steps towards a comprehensible approach to test for the suitability of reference sites.

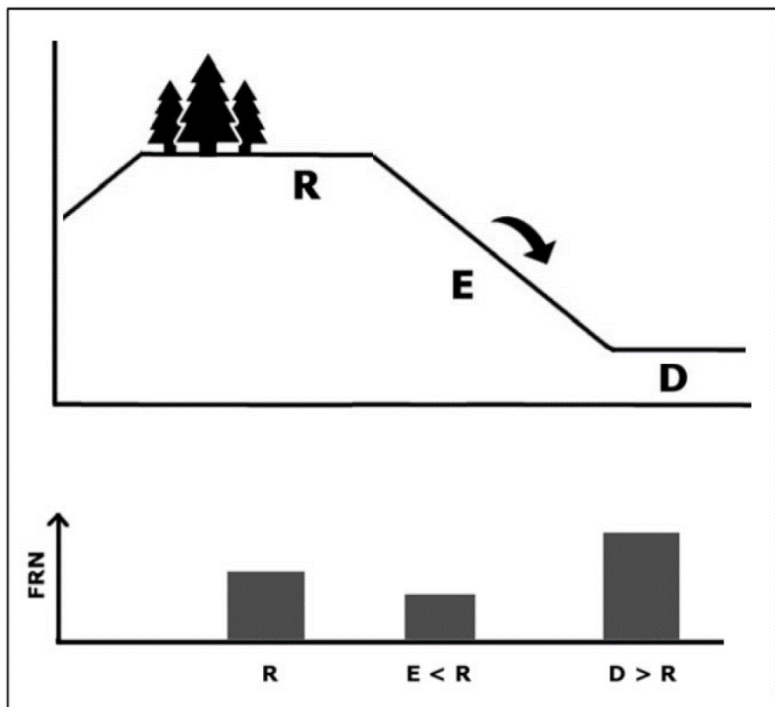
Keywords: FRN, fallout radionuclides, soil degradation,  $^{210}\text{Pb}_{\text{ex}}$ ,  $^{239+240}\text{Pu}$ , comparability of gamma spectrometers, Cesium-137

## 30 1 Introduction

Soil erosion is a global threat (Lal, 2003). Recent estimated erosion rates range from low rates of  $0.001\text{--}2 \text{ t ha}^{-1} \text{ yr}^{-1}$  on flat relatively undisturbed lands (Patric, 2002) to high rates under intensive agricultural use of  $> 50 \text{ t ha}^{-1} \text{ yr}^{-1}$ . In mountainous

regions, rates ranging from 1–30 t ha<sup>-1</sup> yr<sup>-1</sup> have been reported (e.g. Descroix et al. 2003, Frankenbergs et al. 1995, Konz et al., 2012) where they often exceed the natural process of soil formation (Aleweli et al., 2015). The use of the artificial radionuclide <sup>137</sup>Cs as soil erosion tracer has been increasing during the last decades, and the method has been applied all over the world with success (e.g. Mabit et al., 2013; Zapata, 2002). The use of <sup>137</sup>Cs as  erosion tracer allows an integrated temporal estimate of the total net soil redistribution rate per year since the time of the main fallout, including all erosion processes by water, wind and snow during summer and winter seasons (Meusburger et al., 2014).

<sup>137</sup>Cs was released  in the atmosphere during nuclear bomb tests and as a consequence of nuclear power plant (NPP) accidents such as Chernobyl in April 1986. It reached the land surface by dry and wet fallouts and once deposited on the ground, it is strongly bound to fine particles at the soil surface. Due to its low vertical migration rates, it moves predominantly in association with fine soil particles through physical processes, and provides an effective track of soil and sediment redistribution processes (Mabit et al., 2008). The traditional approach in using the <sup>137</sup>Cs method is based on the comparison between the inventory (total radionuclide activity per unit area) at a given sampling site and that of a so-called reference site, located in a flat and undisturbed/stable area. The method indicates the occurrence of erosion processes at sites with lower <sup>137</sup>Cs inventory as compared to the reference site, and sediment deposition processes at sites with a greater <sup>137</sup>Cs inventory (Figure 1, A). Specific mathematical conversion models allow then to derive from the latter comparison quantitative estimates of soil erosion and deposition rates (IAEA, 2014).



50 **Figure 1: Concept of the fallout radionuclide (FRN) traditional method, in which the FRN content of a reference site located in a flat and undisturbed area (R) is compared to the FRN content of disturbed sites (E and D). If the FRN at the site under investigation**

is lower than at the reference site, the site has experienced erosion processes (E), while if the FRN content is greater than at the reference site, the site has experienced deposition processes (D).

The efficacy of the method relies on an accurate selection of representative reference sites (Mabit et al., 2008; Owens and 55 Walling, 1996, Sutherland, 1996). The measured total  $^{137}\text{Cs}$  inventory at the reference sites represents the baseline fallout (i.e. reference inventory), a fundamental parameter for the qualitative and quantitative assessment of soil redistribution rates (Loughran et al., 2002). It is used for the comparison with the total  $^{137}\text{Cs}$  inventories of the sampling sites, and  before determines if and how strongly a site is eroding or accumulating sediments. Moreover, the depth profile of the  $^{137}\text{Cs}$  distribution in the soil at the reference site plays a very important role, as the shape of this profile is used in the conversion models to 60 convert changes in  $^{137}\text{Cs}$  inventory changes  quantitative estimates of soil erosion rates (Walling et al., 2002). Recent studies demonstrated the sensitivity of conversion models to uncertainties or even biases in the reference inventory (e.g. Arata et al., 2016; Iurian et al., 2014; Kirchner, 2013).

A close proximity of a reference site to the area under investigation is required to meet the assumption that both experienced 65 similar initial fallout. The latter is particularly important if the study area was strongly affected by Chernobyl fallout, which is, besides global fallout from nuclear weapons testing, the major input of  $^{137}\text{Cs}$  in many regions of Europe. Because of different geographical situations and meteorological conditions  at the time of passage of the radioactive cloud, the contamination associated with Chernobyl fallout was very  inhomogeneous (Chawla et al., 2010, Alewell et al., 2014). Therefore, in some areas a significant small scale variability of  $^{137}\text{Cs}$  distribution may be expected and, as already pointed out by Lettner et al.

(1999) and Owens and Walling (1996), might impede the comparison between reference and sampling sites. To consider 70 adequately the spatial variability of the FRN fallout, multiple reference sites should be selected and the variability within the sites properly tackled (Kirchner, 2013, Mabit et al., 2013, Pennock and Appleby, 2002). In addition, the reference site should not have experienced any soil erosion or deposition processes since the main  $^{137}\text{Cs}$  fallout (which generally requires that it was under continuous vegetation cover such as perennial grass). Different forms of turbation, including animal-, anthropogenic- and cryoturbation or snow processes may also affect the  $^{137}\text{Cs}$  soil depth distribution at the reference site. Finally, the collection

75 of the samples, the preparation process and the gamma analysis might introduce a certain level of uncertainty, which should be carefully considered. For instance, Lettner et al. (1999) estimated that the preparation and measuring processes contribute 12.2% to the overall variability of the reference inventory. Guidance in form of independent indicators (e.g. stable isotopes as suggested by Meusburger et al., 2013) for the suitability of reference sites might help to assist with the selection of  reference sites.

80 All in all the suitability or unsuitability of references site is crucial, maybe even the most crucial step, in all FRN based erosion assessments. The general suitability of  $^{137}\text{Cs}$  based erosion assessment has been recently discussed very controversially (Parsons and Forster 2011, 2013; Mabit et al., 2013). We would like to propose that the FRN community needs to agree on general  aspects and sampling strategies to test the suitability  of reference sites in order to improve the method as well as  establish trust in this useful erosion assessment method. Up  now, the variability among spatial replicate samples at reference sites  commonly the sole criteria to decide on the suitability of a reference value. We propose an extended method to Check



the Suitability of reference Sites (CheSS) using a repeated sampling strategy and as such an assessment of the temporal variability of reference sites. The suitability of reference sites for an accurate application of  $^{137}\text{Cs}$  as soil erosion tracer is tested at Urseren Valley (Canton Uri, Swiss Central Alps).

## 90 2 CheSS (Check the Suitability of reference Sites): a concept to assess the suitability of reference sites for application of $^{137}\text{Cs}$ as soil erosion tracer

### 2.1 Repeated sampling strategy and calculation of inventories

The time period for the repeated sampling of reference sites needed for the application of  $^{137}\text{Cs}$  as soil erosion tracer will be site specific and depends on the initial small scale spatial variability and the depth distribution of the reference inventory. The time span should be of sufficient length to cause an inventory change that is larger than the uncertainty related to the inventory assessment e.g. larger than 5%. In our study site being effected by anthropogenic disturbance and snow erosion of several mm per winter already 2 years can be considered sufficient (Meusburger et al., 2014). Several spatial repetitions following the suggestion of Sutherland et al. (1996) are necessary and should be analysed separately to investigate the small scale variability of  $^{137}\text{Cs}$  in the area. As we detected measurement differences between different detectors (see below), all samples should ideally be measured for  $^{137}\text{Cs}$  activity using the same analytical facilities. Finally,  $^{137}\text{Cs}$  activity needs to be decay corrected to the same date (either the period of the first sampling campaign or the second one), considering the half-life of  $^{137}\text{Cs}$  (30.17 years).

The decay corrected  $^{137}\text{Cs}$  activities ( $act$ ,  $\text{Bq kg}^{-1}$ ), of each soil layer of the depth profile are converted into inventories ( $inv$ ,  $\text{Bq m}^{-2}$ ) with the following equation:

$$100 Inv = act \times xm \quad (1)$$

105 where  $xm$  is the measured mass depth of fine soil material (<2 mm fraction) ( $\text{kg m}^{-2}$ ) of the respective soil sample. The depth profile of each reference site is then displayed as inventory ( $\text{Bq m}^{-2}$ ) against the depth of each layer (cm). The repeated-sampling inventory change ( $Inv_{change}$ ) can then be defined as:

$$110 Inv_{change} = \frac{Inv_{t0} - Inv_{t1}}{Inv_{t0}} \times 100 \quad (2)$$

where  $t_0$  and  $t_1$  are the dates of the first and the second sampling campaigns respectively,  $Inv_{t1}$  is the  $^{137}\text{Cs}$  inventory ( $\text{Bq m}^{-2}$ ) at  $t_1$ , and  $Inv_{t0}$  is the  $^{137}\text{Cs}$  inventory at  $t_0$ . Positive values of  $Inv_{change}$  indicate erosion, whereas negative values stand for deposition.

### 2.2 A decision tree to assess the suitability of reference sites



We evaluated the suitability of the reference sites by analyzing in addition to the spatial variability the temporal variation of the  $^{137}\text{Cs}$  inventory. Given the assumption that no additional deposition of  $^{137}\text{Cs}$  occurred at the sites during the investigated

115 time window (which is valid worldwide except for the areas affected by the Fukushima-Daiichi fallout), any temporal variation of the  $^{137}\text{Cs}$  content should be attributable to different forms of soil disturbance or to artefacts in the preparation/measurement of the samples. The potential causes of the spatial and temporal variation in the  $^{137}\text{Cs}$  total inventories and depth profiles are examined through a decision tree which includes three main nodes (Figure 2).

#### Node 1: Spatial variation of FRN total inventory

120 Firstly, the spatial variation of the  $^{137}\text{Cs}$  total inventory at each reference site is tested. Ideally, several replicates have been collected. If the coefficient of variation (CV) exceeds 35% as suggested by Sutherland (1996), this could be a sign of unsuitability of the reference site, baves the possibility of i) increasing sampling numbers, ii) analysing the causes for the spatial variation (see CheSS A to D) and iii) moving to node 2 and 3 in CheSS.

#### Node 2: Variation of the $^{137}\text{Cs}$ depth profile

125 Secondary, it is tested whether there is a significant variation between the  $^{137}\text{Cs}$  depth profiles measured as spatial or temporal (in  $t0$  and  $t1$ ) replicates. In theory, at a stable site shape of the depth profile should not change between replicates. Consequently, a regression between the FRN activity depth profiles collected as spatial or temporal replicates should follow a 1:1 line and the variability should lie within the range of the observed spatial uncertainty (node 1). A deviation of the linear regression coefficient from the 1:1 line in combination with high residues and low  $R^2$  values ( $<0.5 R^2$ ) indicates an immediate 130 and significant change of the profile, which is typically caused by anthropogenic disturbance. For the FRN application at ploughed sites reference site might still be considered appropriate if the total inventory is not affected, because conversion models used for ploughed are less sensitive to the of the FRN depth distribution. For unploughed soils again the analysis of the causes A to D might help to understand the causes for the variability. Alternative options would be to take temporal replicates to evaluate the stability and thus suitability of the reference site (node 3).

#### 135 Node 3: Temporal variation of FRN total inventory

If the CV of all replicates taken in  $t0$  and  $t1$  is  $<35\%$ , the reference site might be used for the FRN method. The longer the time period between the first and second sampling is the more reliable the yielded assessments will be. Further a suitable test for significant differences should confirm or reject the hypothesis of  $^{137}\text{Cs}$  total inventory stability over time. If the potential causes for variation (A to D) do not apply, the site is not suitable for the traditional FRN approach. Still a repeated sampling approach 140 could be used to assess soil redistribution rates based on FRN methods (Porto et al., 2014; Kachanowski & de Jong, 1984).

## Analysis of the SPATIAL and/or of the TEMPORAL variation

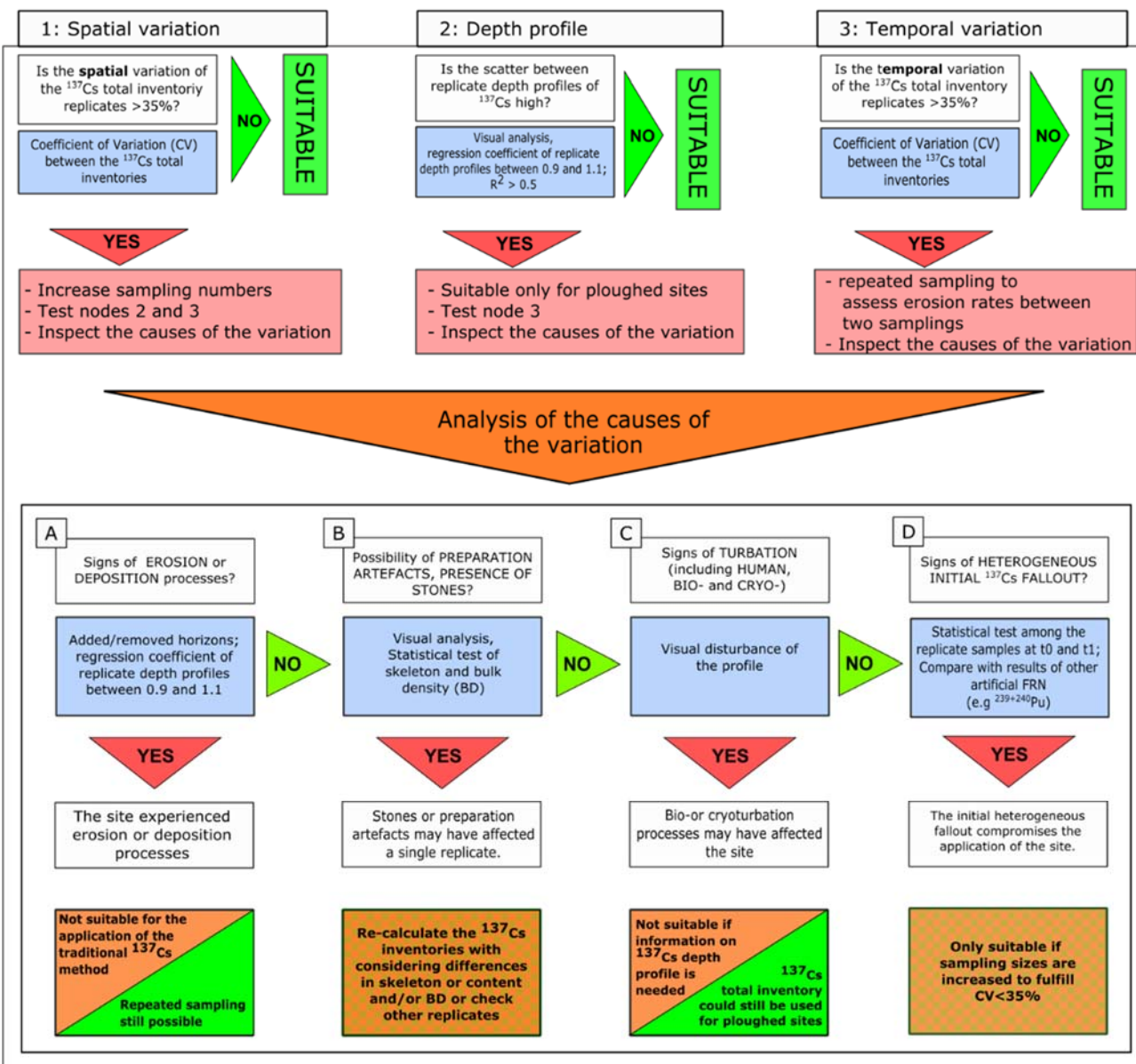


Figure 2: The CheSS decision tree to evaluate the suitability of a reference site for using  $^{137}\text{Cs}$  as an erosion tracer.

### A: Signs of disturbance associated with erosion and deposition processes

145 A variation in the  $^{137}\text{Cs}$  depth profile may have been caused by soil movement processes affecting the site (Figure 2, A). If the site experienced a loss of soil due to erosion, we expect to observe a removal of the top soil layers of the profile measured for

instance during the second sampling campaign (Figure 3, red values below the reference profile). Further, the regression coefficient of the reference site that was affected by erosion will tend to be  $<0.9$  when plotted against a suitable reference profile or (for node 3) the reference profile before the disturbance (Figure 3). In case of deposition, a sedimentation layer 150 should be found on the top of the reference depth profile, assuming that no ploughing operations affected the site (Figure 3, red values above the reference profile). In this case, the regression coefficient will be  $>1.1$ . Information on the depth distribution of another FRN might provide additional reliable confirmation. If redistribution processes are confirmed the site is not suitable as a reference site and other location or a repeated FRN sampling approach to estimate erosion rates between the two sampling campaign should be considered (Kachanoski & de Jong, 1984).

reference	deposition	erosion
34	27	17.6
30	33	19.4
17.6	34	10
19.4	30	9.3
10	17.6	10.2
9.3	19.4	9.3
10.2	10	5
9.3	9.3	4.2
5	10.2	1
4.2	9.3	1

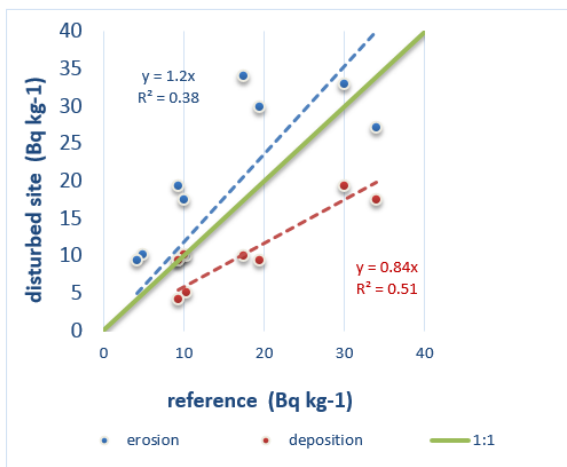


Figure 3: Signs of sheet erosion (A) and deposition (B) on a depth profile of a hypothetical reference site.

## B: Sampling or preparation artefacts

One very common artefact which might bias the comparison between the samples collected at different sites or at  $t0$  and  $t1$  is the difference in skeleton content (the percentage of soil fractions  $>2\text{mm}$ ) (Figure 2, B). The presence of stones might 160 determine pass ways of water as well as fine particles and solutes in and thus influence the accumulation/migration of  $^{137}\text{Cs}$  through the soil layers. As  $^{137}\text{Cs}$  reaches the soil by fallout from the atmosphere, the common shape of the  $^{137}\text{Cs}$  distribution along the undisturbed depth profile can be described by an exponential function, with the highest

<sup>137</sup>Cs concentrations located in the uppermost soil layers (Mabit *et al.*, 2008; Walling *et al.*, 2002). This is particularly the case for soils with low skeleton content (Figure 4, A) since the presence of stones may affect <sup>137</sup>Cs depth distribution either through (i) impeding the <sup>137</sup>Cs downward migration (<sup>137</sup>Cs activity could then be concentrated in the layer above the stone (Figure 4, B) or (ii) creating macro- and micro-pores favouring <sup>137</sup>Cs associated with fine particles to “migrate” to deeper layers (Figure 4, C) or causing lateral movement which will induce a lower <sup>137</sup>Cs content in our samples.

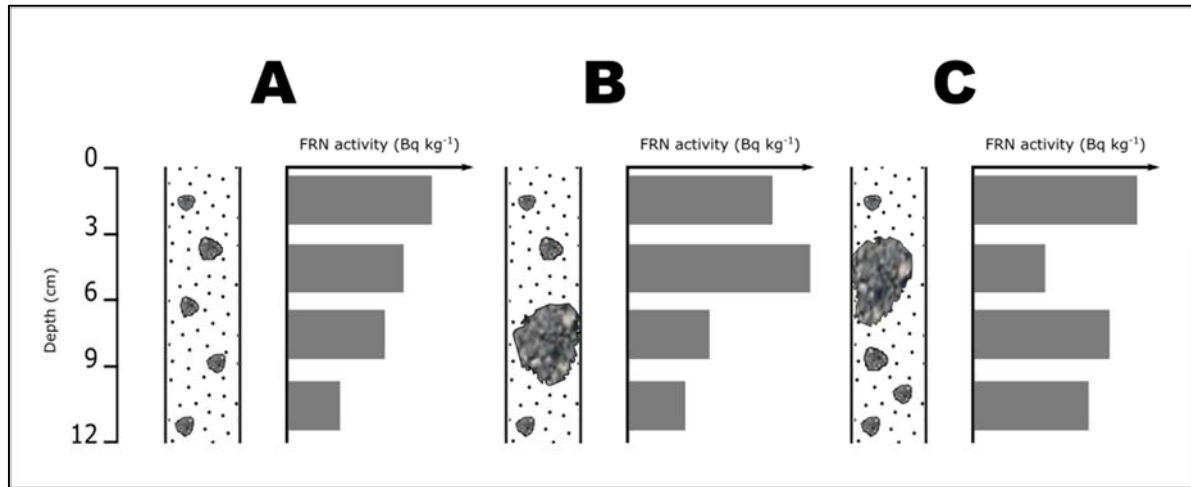


Figure 4: Possible influence of stones on the FRN depth distribution.

As such, the seemingly spatial or temporal variation in the depth profile might indeed be a spatial variation induced by differences in skeleton content and/or bulk densities. Higher bulk densities will result in higher increment inventories even if <sup>137</sup>Cs activities at different layers are comparable. Thus, a thorough control (eventually through a statistical test such as paired T-test) if skeleton content and bulk densities are comparable between replicates is suggested. Finally, sampling, preparation artefacts and measuring processes may produce various sources of errors between different sites and years. The latter is especially the case, if different people prepared the samples. An estimation of possible errors might be considered, for example through a simulation of different increment assignments along the profile. If different detectors or different calibration sources and/or geometries used in the two sampling campaigns, a comparability check of the measurements is advisable. For instance, a subset of samples could be measured with the two different detectors and any potential discrepancy of the results should be properly reported.

### 180 C: Signs of soil disturbance

Different forms of disturbance, such as bio-, cryoturbation or even human induced soil perturbation (e.g. tillage, seed bed preparation, digging etc.) might have influenced the <sup>137</sup>Cs depth distribution between different sites and *t0* and *t1* (Figure 2, C). Occurrences of disturbance are often difficult to identify prior to sampling but might eventually be detected by using other tracing approaches, such as the  $\delta^{13}\text{C}$  depth distribution (Meusburger *et al.*, 2013; Schaub and Alewell, 2009). In case of

185 turbation the shape of the depth profile will be highly variable and should not be considered in the estimation of soil redistribution rates for unploughed soils. Nonetheless, the total inventory of  $^{137}\text{Cs}$  at a ploughed site could still be used in combination with simple and basic mathematical conversion models, such as the proportional model (Ritchie and McHenry, 1990, IAEA, 2014), which require information only  about the total reference inventory of  $^{137}\text{Cs}$ , and do not need detailed information about the  $^{137}\text{Cs}$  depth distribution.

190 **D: Signs of a heterogeneous initial fallout of  $^{137}\text{Cs}$  over the area**

Finally  significant difference between reference replicates may be caused by a high small scale spatial variability of  $^{137}\text{Cs}$  distribution at the site, due to heterogeneous initial fallout over the study area (Figure 2, D). In Europe, significant small scale variability of  $^{137}\text{Cs}$  distribution is known to be due to the Chernobyl fallout, which was characterized by a high  $^{137}\text{Cs}$  deposition associated with few rain events. Compared to the nuclear bomb tests fallout, the Chernobyl fallout was significantly more 195 heterogeneous (e.g. Alewell *et al.*, 2014). Therefore, in the areas affected by the Chernobyl fallout, sites sampled close  to each other may present very different  $^{137}\text{Cs}$  contents. It is therefore necessary to investigate the small scale spatial variability (e.g. the same scale as distance between reference site replicates) measured at both or at least one sampling campaign, looking 200 at the CV again, as presented in the previous sections, or through a statistical test (for example the Analysis of the Variance, ANOVA). If the spatial variability is highly significant, the site should not be envisaged as a reference site for the application of the  $^{137}\text{Cs}$  method unless the number of samples collected for the determination of the reference baseline is large enough (at least 10) to counterweight the small scale variability within the site (Mabit *et al.*, 2012; Sutherland, 1996, Kirchner, 2013). A possible validation of this cause of heterogeneity might be a comparison with the spatial distribution of another FRN such as 239+240Pu or  $^{210}\text{Pb}_{\text{ex}}$  (Porto *et al.*, 2013). (Figure 2, D). As the fallout deposition of  $^{239+240}\text{Pu}$  after the Chernobyl accident was 205 confined to a restricted area in the vicinity of the Nuclear Power Plant (Ketterer *et al.*, 2004), the origin of Plutonium fallout in the rest of Europe is linked to the past nuclear bomb tests only. Consequently, Pu fallout distribution was more homogeneous (Alewell *et al.*, 2014; Ketterer *et al.*, 2004; Zollinger *et al.*, 2015). If the  $^{239+240}\text{Pu}$  depth profiles do not vary significantly between the two sampling years, there should be no disturbance (e.g. turbation, erosion) or measurement artefacts. As such, it might be concluded that the heterogeneous deposition of  $^{137}\text{Cs}$  at the time of the fallout prejues the use of Cs at this site.

### 3 The application of the CheSS decision tree

210 **3.1 Study area**

To test the methodology described above, we used a dataset from an alpine study area, the Urseren Valley ( $30 \text{ km}^2$ ) in Central Switzerland (Canton Uri), which has an elevation ranging from 1440 to 3200 m a.s.l. At the valley bottom (1440  a.s.l.), average annual air temperature for the year  1980–2012 is around  $4.1 \pm 0.7 \text{ }^{\circ}\text{C}$  and the mean annual precipitation is  $1457 \pm 290 \text{ mm}$ , with 30% falling as snow (MeteoSwiss, 2013). The U-formed valley is snow-covered from November to April. On 215 the slopes, pasture is the dominant land use, whereas hayfields are prevalent near the valley bottom.

### 3.2 Sampling design

Supportive information was provided by the local landowners to select the reference sites in both valleys. Sites used for ploughing and grazing activities were excluded. A first sampling campaign was undertaken in autumn 2010 for  $^{239+240}\text{Pu}$  and 2013 for  $^{137}\text{Cs}$  reference sites (REF1 to REF6) were identified in flat and undisturbed areas along the valley. At each site 220 3 cores (40 cm depth), apart from each other, were sampled. The cores were cut in increments, to derive information on the  $^{137}\text{Cs}$  depth profile.

The three cores from each site were bulked to provide one composite sample per site. During the second sampling campaign in spring 2015, all six reference sites were resampled. Considering the typical and high soil redistribution dynamics of the valley of >1 cm per year caused by snow induced soil removal (Meusburger et al., 2014), the time span is sufficiently long to ensure the possibility to observe changes in the depth profiles if soil erosion and deposition 225 processes affected the area. At each site, we collected three replicates, which were analyzed separately, to investigate the small scale variability of the FRN content. All cores were air-dried (40°C for 72h), sieved (<2 mm) to remove coarse particles and the skeleton content as well as the bulk density (BD) was determined.

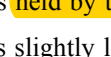
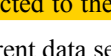
### 3.3 Measurement of anthropogenic FRN activities and inventories

The measurements of the  $^{137}\text{Cs}$  activity (Bq kg $^{-1}$ ) were performed with high resolution HPGe detectors. The  $^{137}\text{Cs}$  activity (Bq 230 kg $^{-1}$ ) in 2013 were analysed at the Institute of Physics of the University of Basel using a coaxial, high resolution germanium lithium detector (Princeton Gammatech) with a relative efficiency of 19% (at 1.33 MeV,  $^{60}\text{Co}$ ). Counting time was set to 24 hours per sample. Samples collected in 2015 were analysed at the state laboratory Basel-City using coaxial high resolution germanium detectors having 25% to 50% relative efficiencies (at 1.33 MeV,  $^{60}\text{Co}$ ). Counting times were set to provide a precision of less than  $\pm 10\%$  for  $^{137}\text{Cs}$  at the 95% level of confidence.

235 All soil samples were counted in sealed discs (65 mm diameter, 12 mm height, 32 cm $^3$ ) and the measurements were corrected for sample density and potential radioactivity background. The detectors located at the state laboratory Basel-City were calibrated with a reference solution of the same geometry. The reference contained  $^{152}\text{Eu}$  and  $^{241}\text{Am}$  (2.6 kBq resp. 7.7 kBq) to calibrate the detectors from 60 to 1765 keV. It was obtained from the Czech Metrology Institute, Prag. This solution was bound in resin with a density of 1.0. The efficiency functions were corrected for coincidence summing of the  $^{152}\text{Eu}$  lines using a 240 Monte Carlo simulation program (Gespecor). The  $^{137}\text{Cs}$  was counted at 662 keV with an emission probability of 0.85 and a (detector) resolution of 1.3 to 1.6 keV (FWHM). All measurements and calculations were performed with the gamma software Interwinner 7. The  $^{137}\text{Cs}$  activity measurements were all decay corrected to the year 2015.

To compare the  $^{137}\text{Cs}$  results with other artificial FRN, all samples were also measured for  $^{239+240}\text{Pu}$  activity. The determination of Plutonium isotopes from both valleys and for both sampling years were performed using a Thermo X Series II quadrupole 245 ICP-MS at the Northern Arizona University, USA. Detailed description of the ICP-MS specifications and sample preparation procedure can be found in Alewell et al., 2014. The activities of  $^{137}\text{Cs}$  and  $^{239+240}\text{Pu}$  (act, Bq kg $^{-1}$ ) were converted into inventories (Bq m $^{-2}$ ) according to equation (1).

### 3.4 Application of the CheSS decision support tool to the reference sites

Because the  $^{137}\text{Cs}$  activity of the samples was measured with different detectors for the two sampling years, we investigated 250 the potential variability between the  detectors. A selected subset of samples (n= 24) was analysed using both detectors (i.e. the one located at the Institute of Physics of the University of Basel and  the other located at the State Laboratory Basel-City). The results highlight a high correspondence of the measurements  held by the two analytical systems ( $R^2 = 0.97$ ;  $p < 0.005$ ), however  the detector of the State Laboratory Basel-City  returns slightly lower  $^{137}\text{Cs}$  activities (Figure 5). Thus, the  $^{137}\text{Cs}$  activities of the samples measured in 2013  were corrected to the values of the detector of State Laboratory Basel-City 255 (higher efficiency) to allow comparability between the different data sets.

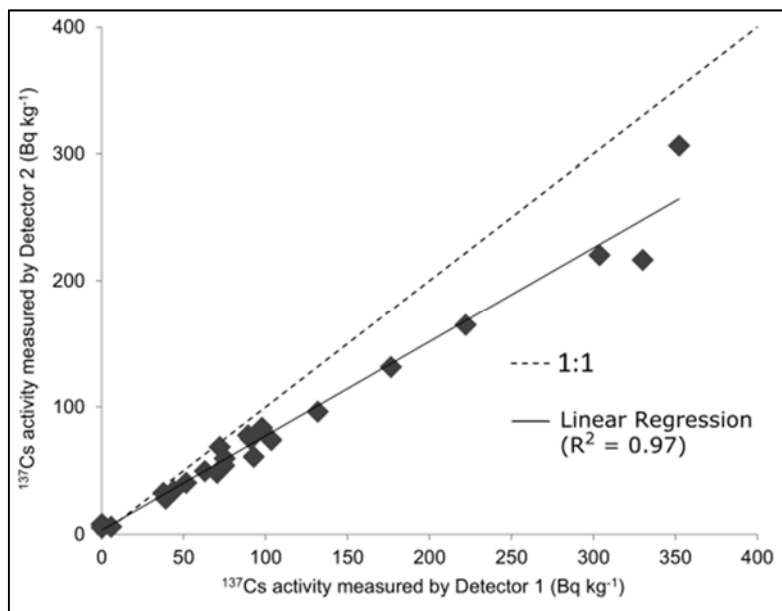
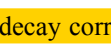
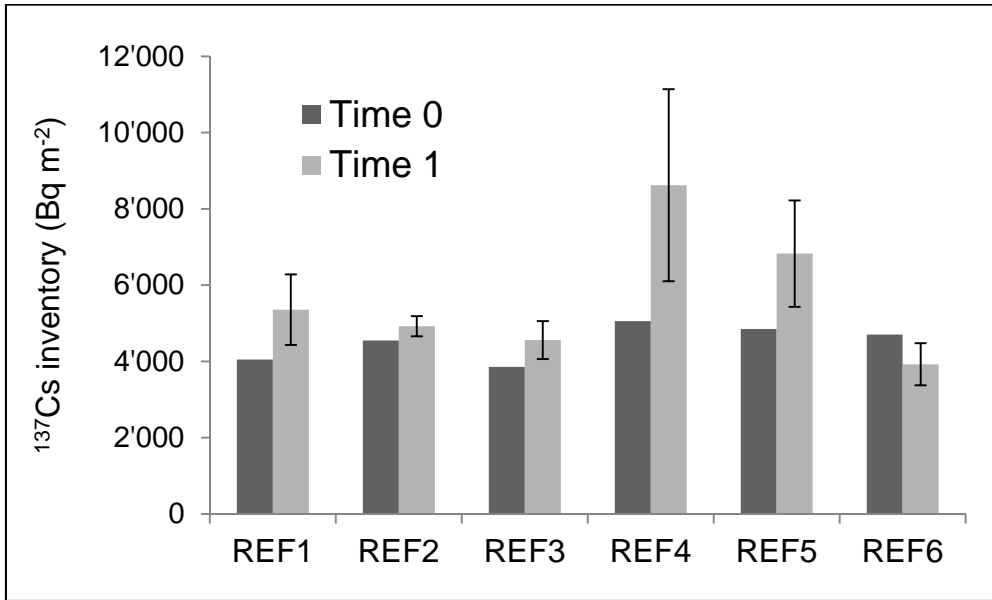


Figure 5: The comparison between the  $^{137}\text{Cs}$  measurements of a subset of samples (n=16) performed with two different HpGe detectors, where detector 1: detector hosted at the Physics department of the University of Basel (CH) and detector 2: detector hosted at the State-Laboratory of Basel (CH).

260 Total  $^{137}\text{Cs}$  inventories  (decay corrected) to the  of the six reference sites collected in the Urseren Valley in 2013 ranged  between 3858 to 5057  $\text{Bq m}^{-2}$ , with a mean value of 4515  $\text{Bq m}^{-2}$  and a standard deviation (SD) of 468  $\text{Bq m}^{-2}$ . Data from 2015 ranged  between 3925 to 8619  $\text{Bq m}^{-2}$ , with a mean value of 5701  $\text{Bq m}^{-2}$  and a SD of 1730  $\text{Bq m}^{-2}$  (Figure 6).



**Figure 6: Temporal variation between the total  $^{137}\text{Cs}$  inventories measured at the reference sites in the Urseren Valley, where Time 265 0 = 2013 and Time 1 = 2015. The errors bars indicate the standard deviations of the inventories among the replicates collected at each reference 270 site 15.**

When following the CheSS decision tree, we investigated the variation in the  $^{137}\text{Cs}$  total inventories at each reference site (node 1). The replicate samples were analyzed separately only during the second sampling campaign (t1), while during the first sampling campaign (t0) only composite samples were analysed. Reference sites 3, 5 and 6 presented signs of high small scale 270 variability, as expressed by 275 of 48 % (Table 1). Such variability excluded them from any further application as reference sites without subsequent additional sampling. For reference sites 1, 2 and 4, the CV was between 19 – 31%.

Passing to node 2 of the CheSS decision tree, the analysis focused on the variation of the shape of the  $^{137}\text{Cs}$  depth profile (Figure 7). Here 280 examined the regression between the reference depth profiles in t0 and t1. For the three sites with acceptable spatial variability (i.e. reference site 1, 2 and 4) the site REF4 showed signs of deposition with a regression coefficient between t0 and t1 = 1.34. The deposition was confirmed by field observation of construction works that were conducted between the two samplings. After this disturbance, site is not a suitable reference site anymore. Among the sites with high spatial variability REF6 showed signs of erosion with a regression coefficient between t0 and t1 = 0.79.

In node 3 temporal differences in total inventories between t0 and t1 were assessed. Here REF4 showed a significant difference of the total  $^{137}\text{Cs}$  inventories between t0 and t1. Thus, confirming the unsuitability of the site the construction 280 works.

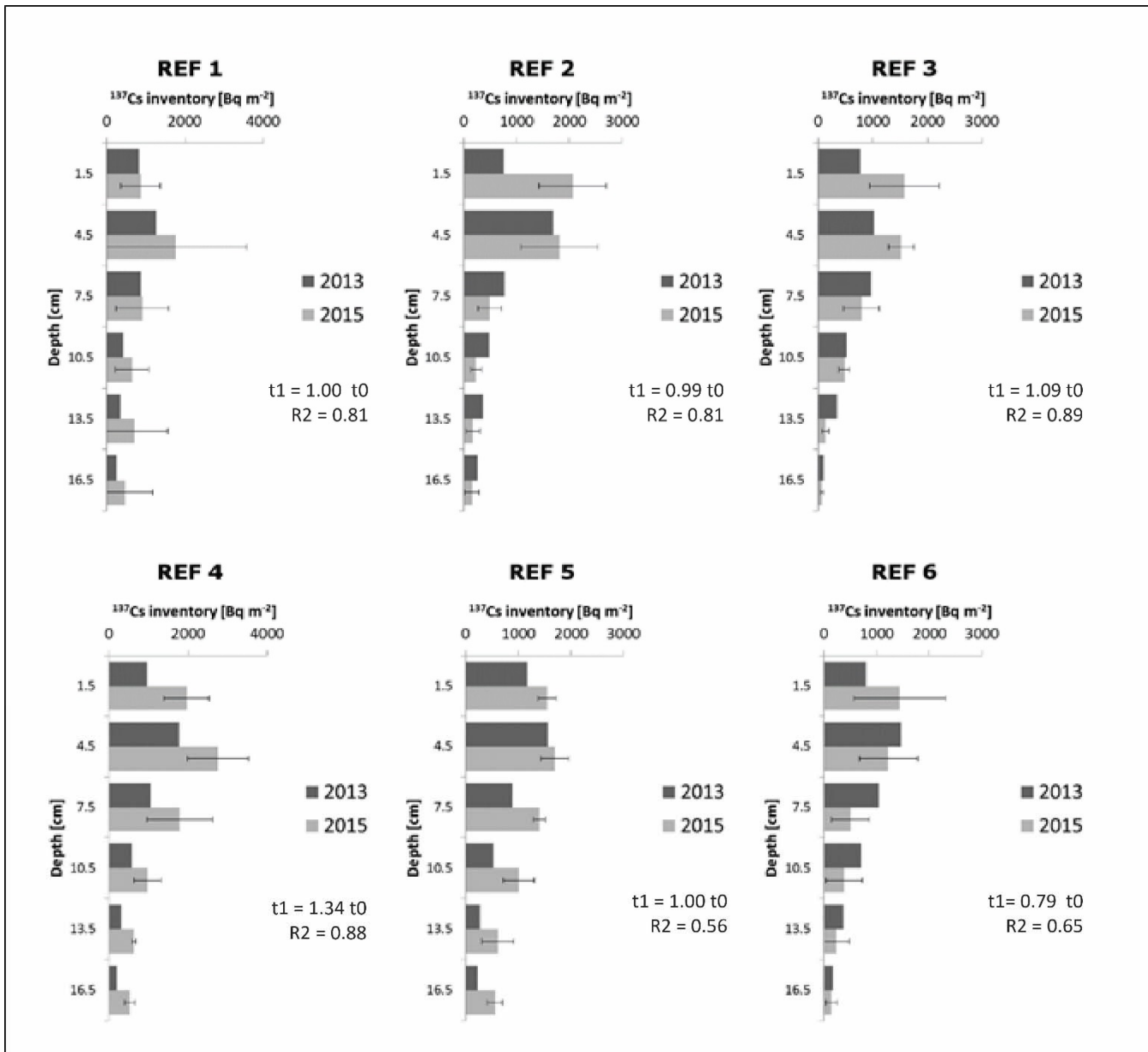
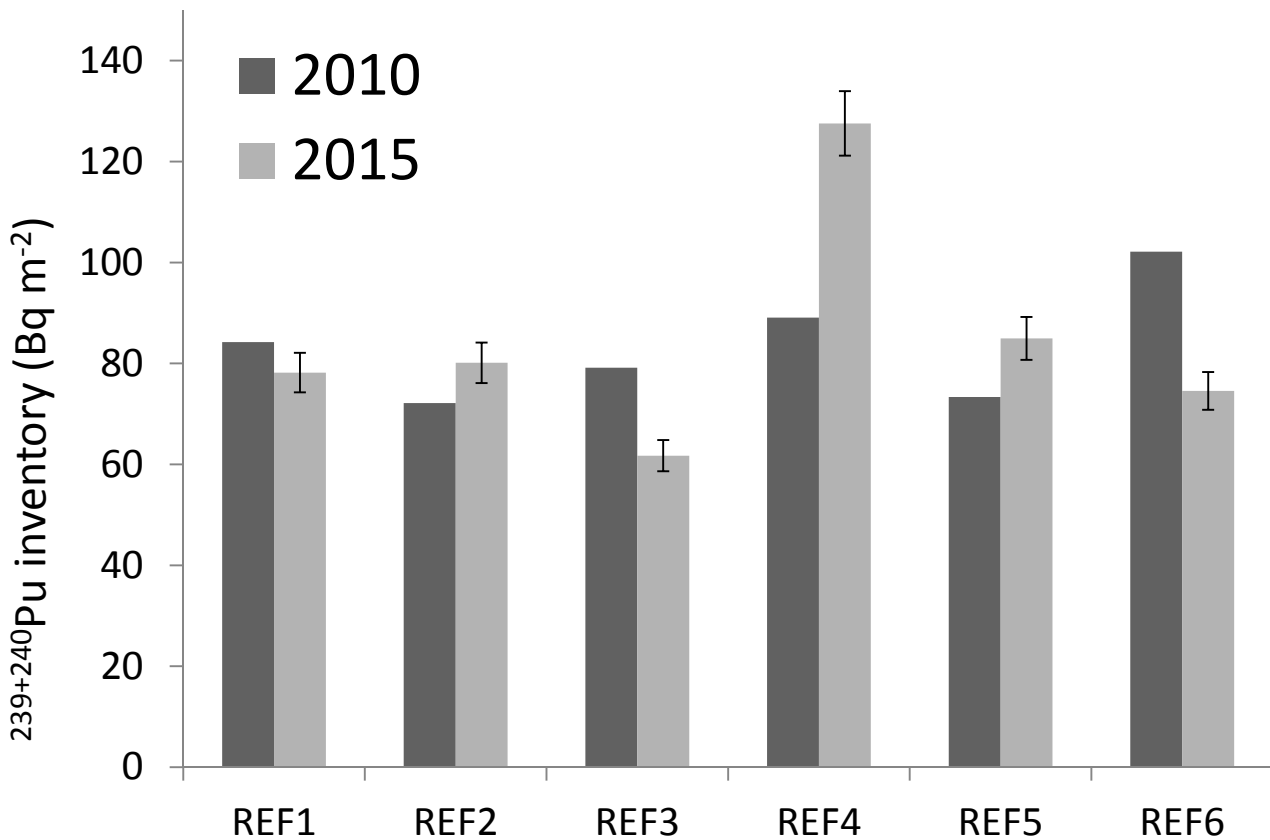


**Figure 7:** The  $^{137}\text{Cs}$  depth profiles of the six investigated reference sites in the Urseren Valley for the two different sampling campaigns. The errors bars indicate the standard deviations of the inventories among the replicates collected at each reference site 5. Furthermore, the regression equation between the depth profile at  $t_0$  and  $t_1$  is displayed together with the  $R^2$ .

285

To further investigate the causes for the spatial variation,  $^{239+240}\text{Pu}$  inventories measured at the three replicates of each site were analysed for  $t_0 = 2010$  and  $t_1 = 2015$  (Figure 8). Clearly deposition for REF4 and erosion processes for REF6 were confirmed with an increase of 46% and a decrease of 27% in the total  $^{239+240}\text{Pu}$  inventory between  $t_0$  and  $t_1$ , respectively.



290

**Figure 8: Temporal variation between the total  $^{239+240}\text{Pu}$  inventories measured at the reference sites in the Urseren Valley, where Time 0 = 2010 and Time 1 = 2015. The errors bars indicate the standard deviations of the inventories among the replicates collected at each reference.**

295 Further, the depth profiles of the three replicates at reference site 1 presented significant differences. We then looked at the differences in the skeleton content of the three replicates (Figure 2, B). An ANOVA test showed a significant difference (p-value of 0.025), thus, a difference in the presence of stones in the three soil cores might have affected the FRN depth distribution. In particular, Tukey's HSD (Honest Significant Difference) Post-hoc pairwise comparison identified the replicate number 3 at REF1 as a potential outlier. To validate the variability of REF1 replicates should be collected and measured, 300 in order to compare their  $^{137}\text{Cs}$  depth profiles to the results obtained during the first sampling campaign. In summary, REF2, REF4 (before the construction works) seem most suitable for  $^{137}\text{Cs}$ . On visual inspection of the soil profile be could exclude the cause C and consequently the final cause of heterogeneous fallout with high spatial variability (D) applies for the sites

REF3 and REF5. These sites may be suitable for FRNs or for  $^{137}\text{Cs}$  if more samples are collected to constrain the spatial heterogeneity that was introduced by the  $^{137}\text{Cs}$  Chernobyl fallout.

305

## 4 Conclusion

With the decision tree CheSS, a support tool to verify the suitability of reference sites for a  $^{137}\text{Cs}$  based soil erosion assessment is presented. Great attention has to be given to the analysis of the small scale variability of  $^{137}\text{Cs}$  distribution in the reference areas, especially in those regions affected by nuclear accident fallout. To cope with small scale variability, sampling numbers might be increased, or the temporal variation of  $^{137}\text{Cs}$  or another radionuclide, such as  $^{239+240}\text{Pu}$  might be analysed. The CheSS test in the Urseren Valley indicated that the heterogeneity and disturbance of  $^{137}\text{Cs}$  distribution prejudiced the suitability of some reference sites. Additionally, the presence of stones affected the shapes of the depth profile in at least one replicate sample at reference site 1. Including unsuitable reference sites, the application of the traditional  $^{137}\text{Cs}$  approach, based on a spatial comparison between reference and sampling sites, is compromised. To derive soil redistribution rates, a  $^{137}\text{Cs}$  repeated sampling approach should be preferred. This approach is based on a temporal comparison of the FRN inventories measured at the same site in different times (Kachanowski & de Jong, 1984). It doesn't require the selection of reference sites, because the inventory documented by the initial sampling campaign is used as the reference inventory for that point (Porto *et al.*, 2014). Accurate soil erosion assessments especially needed to validate soil erosion modelling, which can help prevent and mitigate soil losses on larger spatial scales. In this context, FRN could play a decisive role, if we are able to overcome its potential pitfalls, especially related to the selection of suitable reference sites. The decision tree CheSS provides a support for effective and comparable reference site testing, which enables to exclude those sites which present signs of uncertainty. With this we are convinced to contribute improving the reliability of the FRN based soil erosion assessments.

### Authors contributions.

L. Arata, K. Meusburger, L. Mabit and C. Alewell designed the concept of the method and analysed the data. A. Bürgi contributed to the collection and preparation of the soil samples, and to the analysis of the data. M. Zehringer measured the  $^{137}\text{Cs}$  activity of the soil samples and analysed the results. M. E. Ketterer measured the  $^{239+240}\text{Pu}$  activity of the soil samples. L. Arata prepared the manuscript with contributions from all co-authors.

## Acknowledgements

330 The authors would like to thank Annette Ramp, Gregor Juretzko, Simon Tresch, Carmelo La Spada and Axel Birkholz for support during field work. This work was financially supported by the Swiss National Science Foundation (SNF), project no. 200021-146018, and has been finalized in the framework of the IAEA Coordinated Research Project (CRP) on “*Nuclear techniques for a better understanding of the impact of climate change on soil erosion in upland agro-ecosystems*” (D1.50.17).

## References

335 Alewell, C., Egli, M., & Meusburger, K. 2015. An attempt to estimate tolerable soil erosion rates by matching soil formation with denudation in Alpine grasslands. *Journal of Soils and Sediments*, 15(6), 1383-1399.

Alewell, C., Meusburger, K., Juretzko, G., Mabit, L., & Ketterer, M. E. (2014). Suitability of  $^{239+240}\text{Pu}$  and  $^{137}\text{Cs}$  as tracers for soil erosion assessment in mountain grasslands. *Chemosphere*, 103, 274-280.

Arata, L., Meusburger, K., Frenkel, E., A'Campo-Neuen, A., Iuran, A.R., Ketterer, M.E., Mabit, L., Alewell, C., 2016b. 340 Modelling Deposition and Erosion rates with RadioNuclides (MODERN) - Part 2: A comparison of different models to convert  $^{239+240}\text{Pu}$  inventories into soil redistribution rates at unploughed sites. *Journal of environmental radioactivity*, 162, 97-106.

Chawla, F., Steinmann, P., Pfeifer, H.R., Froidevaux, P., 2010. Atmospheric deposition and migration of artificial radionuclides in Alpine soils (Val Piora, Switzerland) compared to the distribution of selected major and trace elements. *Science of the Total Environment*, 408(16), 3292-3302.

345 Descroix, L., & Mathys, N., 2003. Processes, spatio-temporal factors and measurements of current erosion in the French southern Alps: a review. *Earth Surface Processes and Landforms*, 28(9), 993-1011.

Frankenberg, P., Geier, B., Proswitz, E., Schütz, J., & Seeling, S., 1995. Untersuchungen zu Bodenerosion und Massenbewegungen im Gunzesrieder Tal/Oberallgäu. *Forstwissenschaftliches Centralblatt vereinigt mit Tharandter forstliches Jahrbuch*, 114(1), 214-231.

350 IAEA (International Atomic Energy Agency), 2014. Guidelines for using Fallout radionuclides to assess erosion and effectiveness of soil conservation strategies. IAEA-TECDOC-1741. IAEA publication. Vienna, Austria. 213 p.

Iurian, A. R., Mabit, L., Cosma, C., 2014. Uncertainty related to input parameters of  $^{137}\text{Cs}$  soil redistribution model for undisturbed fields. *Journal of environmental radioactivity*, 136, 112-120.

Kachanoski, R. G., & De Jong, E., 1984. Predicting the temporal relationship between soil cesium-137 and erosion rate. *Journal 355 of Environmental Quality*, 13(2), 301-304.

Ketterer, M.E., Hafer, K.M., Jones, V.J., Appleby, P.G., 2004. Rapid dating of recent sediments in Loch Ness: ICPMS measurements of global fallout Pu. *Science of the Total Environment*, 322, 221-229.

Kirchner, G., 2013. Establishing reference inventories of  $^{137}\text{Cs}$  for soil erosion studies: methodological aspects. *Geoderma* 211, 107-115.

360 Konz, N., Prasuhn, V., Alewell, C., 2012. On the measurement of alpine soil erosion. *Catena*, 91, 63–71.

Lal, R., 2003. Soil erosion and the global carbon budget. *Environ. Int.* 29, 437–450.

Lettner, H., Bossew, P., Hubmer, A.K., 1999. Spatial variability of fallout Caesium-137 in Austrian alpine regions. *J. Environ. Radioact.* 47, 71–82.

Loughran, R.J., Pennock, D.J., Walling, D.E., 2002. Spatial distribution of caesium-137, in: *Handbook for the Assessment of Soil Erosion and Sedimentation Using Environmental Radionuclides*. Springer, pp. 97–109.

365 Mabit, L., Benmansour, M., Walling, D. E., 2008. Comparative advantages and limitations of the fallout radionuclides  $^{137}\text{Cs}$ ,  $^{210}\text{Pb}_{\text{ex}}$  and  $^{7}\text{Be}$  for assessing soil erosion and sedimentation. *Journal of Environmental Radioactivity*, 99(12), 1799–1807.

Mabit, L., Chhem-Kieth, S., Toloza, A., Vanwalleghem, T., Bernard, C., Amate, J.I., de Molina, M.G., Gómez, J.A., 2012. Radioisotopic and physicochemical background indicators to assess soil degradation affecting olive orchards in southern Spain. *Agric. Ecosyst. Environ.* 159, 70–80.

370 Mabit, L., Meusburger, K., Fulajtar, E., Alewell, C., 2013. The usefulness of  $^{137}\text{Cs}$  as a tracer for soil erosion assessment: A critical reply to Parsons and Foster (2011). *Earth-Science Reviews*, 127, 300–307.

Meusburger, K., Leitinger, G., Mabit, L., Mueller, M.H., Walter, A., Alewell, C., 2014. Soil erosion by snow gliding—a first quantification attempt in a subalpine area in Switzerland. *Hydrology and Earth System Sciences*, 18(9), 3763–3775.

375 Meusburger, K., Mabit, L., Park, J.H., Sandor, T., Alewell, C., 2013. Combined use of stable isotopes and fallout radionuclides as soil erosion indicators in a forested mountain site, South Korea. *Biogeosciences* 10, 5627–5638.

Owens, P.N., Walling, D.E., 1996. Spatial variability of caesium-137 inventories at reference sites: an example from two contrasting sites in England and Zimbabwe. *Appl. Radiat. Isot.* 47, 699–707.

Parsons, A. J. and I. D. L. Foster, 2011. "What can we learn about soil erosion from the use of  $^{137}\text{Cs}$ ?" *Earth Science Reviews* 108: 13.

380 Pennock, D.J., Appleby, P.G., 2002. Site selection and sampling design, in: *Handbook for the Assessment of Soil Erosion and Sedimentation Using Environmental Radionuclides*. Springer, pp. 15–40.

Porto, P., Walling, D.E., Alewell, C., Callegari, G., Mabit, L., Mallimo, N., Meusburger, K., Zehringer, M., 2014. Use of a  $^{137}\text{Cs}$  re-sampling technique to investigate temporal changes in soil erosion and sediment mobilisation for a small forested catchment in southern Italy. *J. Environ. Radioact.* 138, 137–148.

385 Porto P, Walling DE, Callegari G., 2013. Using  $^{137}\text{Cs}$  and  $^{210}\text{Pb}_{\text{ex}}$  measurements to investigate the sediment budget of a small forested catchment in southern Italy. *Hydrological Processes*; 27: 795–806.

Ritchie, J. C., Ritchie, C. A., 2001. Bibliography of publications of Cesium-137 studies related to erosion and sediment deposition. USDA-ARS Hydrology and Remote Sensing Laboratory.

390 Schaub, M., Alewell, C., 2009. Stable carbon isotopes as an indicator for soil degradation in an alpine environment (Urseren Valley, Switzerland). *Rapid Commun. Mass Spectrom.* 23, 1499–1507.

Sutherland, R.A., 1996. Caesium-137 soil sampling and inventory variability in reference locations: A literature survey. *Hydrol. Process.* 10, 43–53.

Walling, D.E., He, Q., Appleby, P.G., 2002. Conversion models for use in soil-erosion, soil-redistribution and sedimentation investigations. In: Zapata, F. (Ed.) *Handbook for the assessment of soil erosion and sedimentation using environmental radionuclides*. Kluwer, Dordrecht. Netherlands. pp. 111–164.

395 Zapata, F. (Ed.), 2002. *Handbook for the assessment of soil erosion and sedimentation using environmental radionuclides* (Vol. 219). Dordrecht: Kluwer Academic Publishers.

Zollinger, B., Alewell, C., Kneisel, C., Meusburger, K., Brandová, D., Kubik, P., Schaller M., Ketterer M., Egli, M., 2014. 400 The effect of permafrost on time-split soil erosion using radionuclides ( $^{137}\text{Cs}$ ,  $^{239+240}\text{Pu}$ , meteoric  $^{10}\text{Be}$ ) and stable isotopes ( $\delta^{13}\text{C}$ ) in the eastern Swiss Alps. *Journal of Soils and Sediments*, 15(6), 1400–1419.